Simulations for e/π Separation for the SHMS Heavy Gas Cherenkov Detector

Matthew Strugari, Dr. Garth Huber[1], Wenliang Li

University of Regina, Regina, SK, S4S 0A2, Canada

August 15, 2016

Abstract

The purpose of this report is to present the SHMS Heavy Gas Cherenkov (HGC) detector Geant4 simulation results pertaining to e/π separation between 1.3GeV/c $\leq p \leq$ 7.2 GeV/c using C_4F_{10} and CO_2. This report assumes that the π/e production ratio at the simulated momenta of p = {1.5GeV/c, 3.0GeV/c, 5.0GeV/c, 7.0GeV/c} is π/e = {230, 20, 0.36, 0.0039} respectively. Based on our study, we recommend using CO_2 at P = 0.50atm.

Fig. 1 presents the Cherenkov threshold pressure (P) vs. the SHMS central momentum (p) for C_4F_{10} and CO_2. The black curve is the recommended operating pressure of the HGC detector for good e/π separation. This operating pressure was determined based on an assumed SHMS momentum acceptance of $\delta = \pm$ 15% in addition to an assumed 10% HGC pressure mis-set. The HGC detector only allows sub-atmospheric pressure operation in its original conguration; thus under no circumstance shall the detector pressure exceed 1atm! The detector pressure must be adjusted depending on the pion momentum in order to obtain e/π separation.

The threshold pressure plots were calculated based on the particle rest mass as well as the refractive index of the gas contained in the HGC. The formulae obtained for the refractive index

[1]huberg@uregina.ca

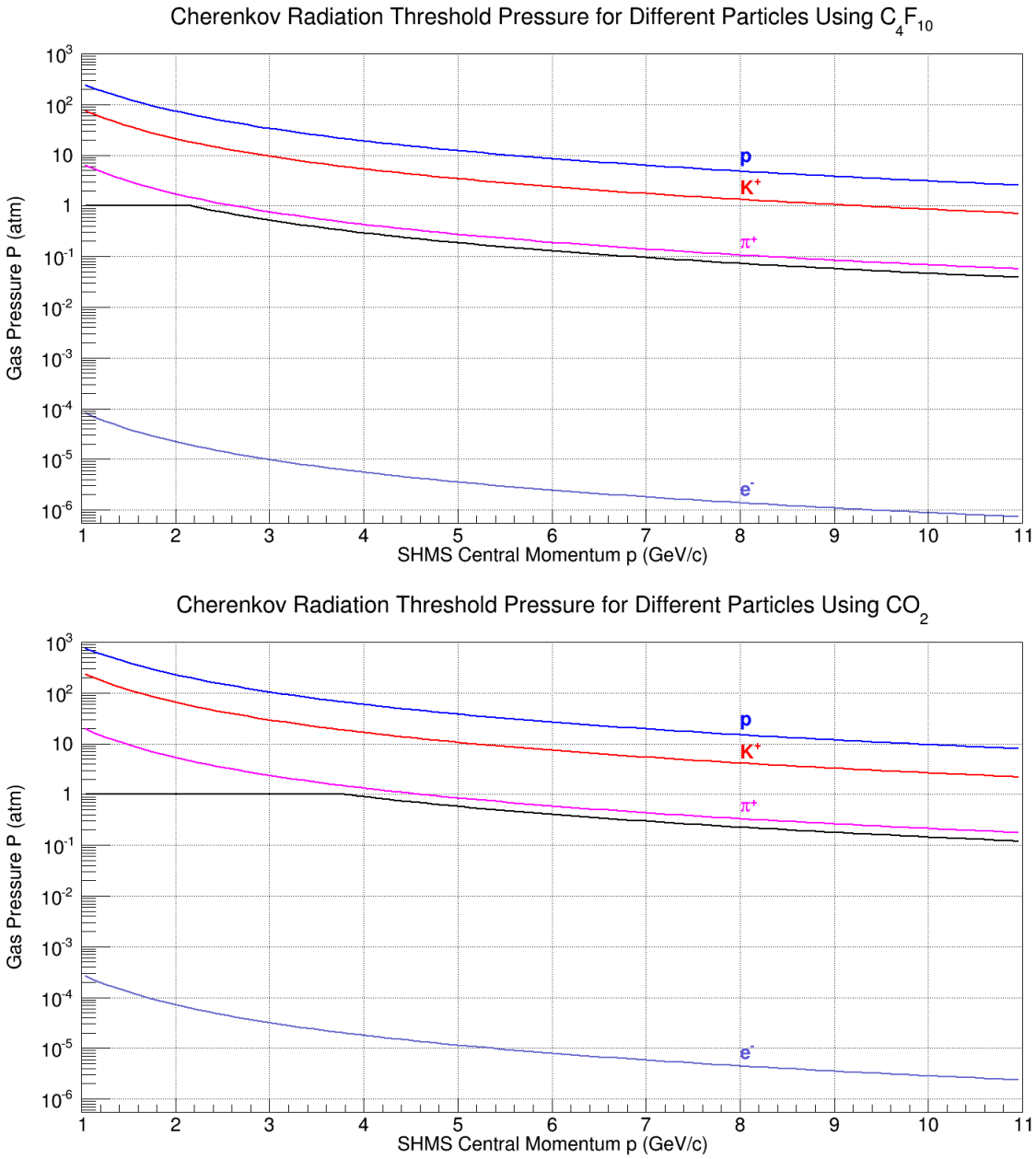

Figure 1: Gas Pressure vs. Particle Momentum. The black curve represents the suggested gas pressure of the HGC detector for good e/π separation. The coloured curves represent the Cherenkov threshold pressure for different particles.

were for a fixed temperature and pressure of T = 0^{o}C and P = 1atm respectively. At a wavelength of 400nm, the index of refraction for C_4F_{10} is n_{1atm} = 1.001424 whereas the index of refraction for CO_2 is n_{1atm} = 1.000459. The wavelength dependent formulae were also implemented in Geant4 to properly simulate the gas contained within the HGC.

The original detector simulation platform for Geant4 was developed at the University of Virginia. Numerous parameters have been implemented to accurately model the components of the HGC. This includes the vessel structure, mirror alignment and radii of curvature, PMT photocathode dimensions and efficiency characteristics, and the optics arrangements. Also, materialistic properties were used to accurately model the HGC components such as the atomic composition, reflectivity, photon absorption length, and refractive index. Additional functions related to Cherenkov radiation were implemented in Geant4 such as the production and tracking of secondary particles. It is essential to model secondary particles since sub-threshold particles can produce a signal due to knock-on electrons.

Geant4 was configured to run multiple simulations over a range of pressure and momenta which produced a realistic estimate of the performance of the HGC for e/π separation. The simulated momenta included $p = \{$1.5GeV/c, 3.0GeV/c, 5.0GeV/c, 7.0GeV/c$\}$ and the pressures ranged from 0.25atm $\leq P \leq$ 0.95atm for C_4F_{10} and 0.25atm $\leq P \leq$ 0.75atm for CO_2. The simulations employed a particle sample size of 200000 which were run separately for the electron and pion. Results were later modified using π/e ratios extrapolated from plots presented in "E12-10-002 and E12-10-008/E12-06-105 Commissioning Experiments" by Simona Malace. The extrapolated π/e ratios for carbon at the aforementioned momenta are presented in Table 1. The ratios from the carbon target were chosen as a "worst case scenario" due to their slightly larger values when compared to the ratios from the hydrogen target.

Fig. 2 (a)-(d) presents the simulated particle event distributions for C_4F_{10} at P = 0.25atm. The blue histogram represents the distribution for the number of detected photo-electrons (p.e.) for 200000 electron events whereas the red histogram represents the distribution for the number of

Momentum p (GeV/c)	π/e Ratio	Angle θ (deg)
1.5	230	35
3.0	20	20
5.0	0.36	17
7.0	0.0039	17

Table 1: Extrapolated π/e ratios for carbon at the simulated momenta

detected p.e. for the scaled (detected pion events $\times$ π/e ratio) pion events. From our simulation, at P = 0.95atm and p = 7GeV/c (not shown) the average p.e. per electron event is 54 and the full width at half maximum (fwhm) is 33 p.e. In Fig. 2 (a)-(d), it can be seen that the average number of detected p.e. is 17 with a fwhm of 9 p.e. There is no significant change in the shape of the distribution from P = 0.95atm to P = 0.25atm. However, the average number of detected p.e. has decreased significantly from 54 to 17. At P = 0.25atm, the false pion detection distribution spreads across 20 p.e. which exceeds the average detected p.e. of 17 for the electron events.

One needs to evaluate the electron inefficiency in addition to the false pion detection efficiency to optimize the detector performance in order to perform e/π separation. The electron detection inefficiency is calculated as:

$$i_e = 1 - \frac{\int_i^{500} dx_{npe}}{200000} \tag{1}$$

and the false pion detection efficiency due to knock-on electrons is calculated as:

$$e_\pi = \frac{\int_i^{500} dy_{npe}}{200000} \tag{2}$$

where x is the detected electron events per p.e. bin, y is the detected pion events per p.e. bin, i is the p.e. threshold, and the upper integral limit of 500 indicates the last histogram bin of our p.e. distribution. We computed the electron detection inefficiency and false pion detection inefficiency for every threshold position and plotted them together as seen in Figs. 2 through 5 (e)-(h). This allowed for the determination of the optimal threshold cut which is defined as the point where the pion and electron curves intersect on the scaled figure. It should be noted that there are two sources

of p.e. detection inefficiency when referring to the detected events: (1) the missed pion or electron events due to optical mis-focussing, absorption, etc. which is independent of the p.e. threshold cut; and (2) the events which occur below the p.e. threshold cut.

Our goal is to achieve greater than 98% electron detection efficiency with the least amount of false pion detection efficiency possible (less than 1.5%). Note that in Fig. 2 (e) the optimal threshold cut at 9.2 p.e. yields 96.7% electron detection efficiency with 3.3% false pion detection efficiency which is lower than our target efficiency. See Fig. 3 for comparison of the simulations with C_4F_{10} at P = 0.50atm. This rules out the possibility for the use of C_4F_{10} at $P \geq$ 0.25atm to perform e/π separation for $p <$ 3GeV/c with the HGC detector. A lower detector operating pressure is needed to achieve good e/π separation. However, the average detected p.e. will decrease. From our calculations, the Cherenkov threshold momentum for pion events in C_4F_{10} at P = 0.25atm is p = 4.6GeV/c. The pion p.e. distribution (red) shown in Fig. 2 (a)-(b) is a result of the delta radiation created by a knock-on electron induced by a sub-threshold pion event. (c)-(d) of Fig. 2 displays the primary Cherenkov radiation distribution produced by above-threshold pion events.

Moving to the CO_2 simulations, as shown in Fig. 4 (a)-(d), the average detected p.e. for each electron event is 10 and the fwhm is 6 p.e. The false pion detection distribution spreads across 10 p.e. compared to 20 for the C_4F_{10} results at P = 0.25atm. It can also be seen that the width of the electron detection distribution is narrower than that of C_4F_{10}. Fig. 4 (e)-(h) shows that for all four simulated momenta, an electron detection efficiency exceeding 99% is achieved. The false pion detection efficiency is less than 0.3% for 3GeV/c, 5GeV/c, and 7GeV/c while for 1.5GeV/c it is 1.0%. Compared to the simulation for CO_2 at P = 0.75atm in Fig. 5, an electron detection efficiency exceeding 98.5% is achieved for all four simulated momenta at P = 0.75atm. Similarly, the false pion detection efficiency is less than 1.5% for 1.5GeV/c and 5GeV/c while for 3GeV/c and 7GeV/c it is less than 0.4%. We recommend a cut at 3.6 p.e. to achieve the optimal electron detection efficiency and false pion detection efficiency for all momenta at an operating pressure of P = 0.50atm.

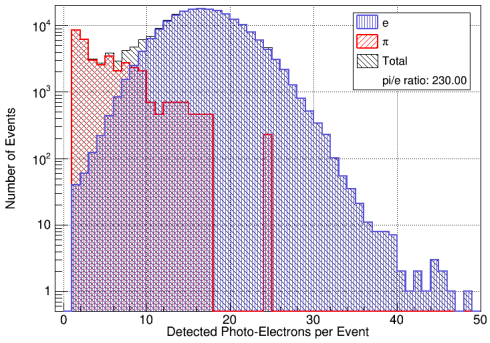

(a) C_4F_{10} @ P = 0.25atm & p = 1.5GeV/c

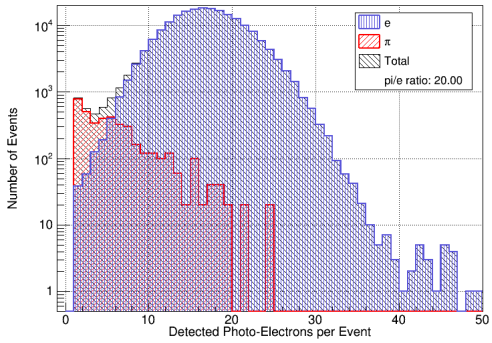

(b) C_4F_{10} @ P = 0.25atm & p = 3GeV/c

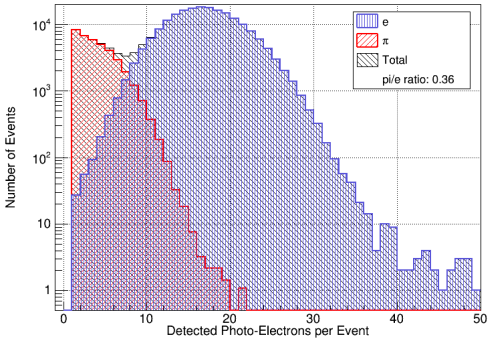

(c) C_4F_{10} @ P = 0.25atm & p = 5GeV/c

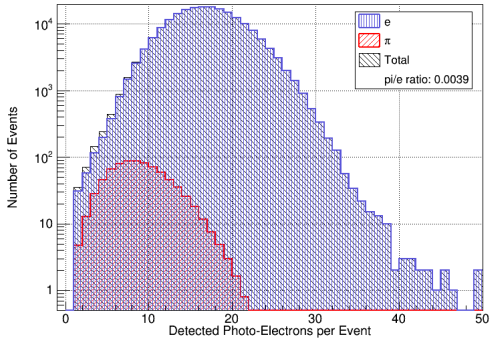

(d) C_4F_{10} @ P = 0.25atm & p = 7GeV/c

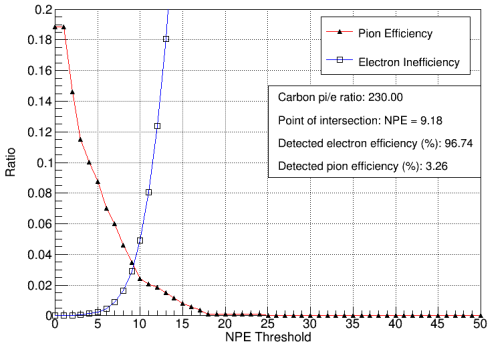

(e) C_4F_{10} @ P = 0.25atm & p = 1.5GeV/c

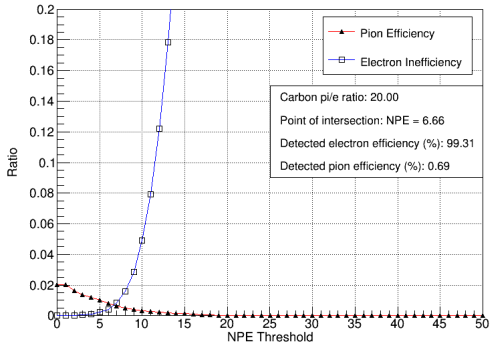

(f) C_4F_{10} @ P = 0.25atm & p = 3GeV/c

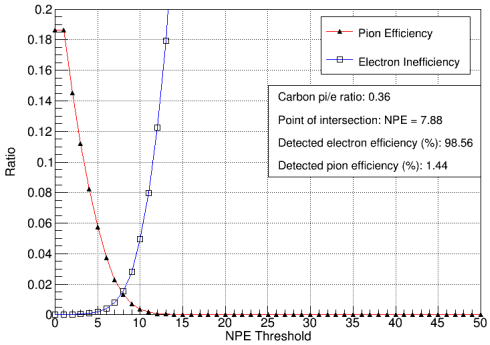

(g) C_4F_{10} @ P = 0.25atm & p = 5GeV/c

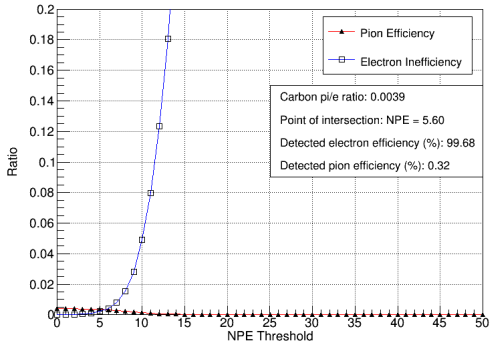

(h) C_4F_{10} @ P = 0.25atm & p = 7GeV/c

Figure 2: (a)-(d) Scaled particle event distribution. The blue distribution represents the detected p.e. distribution for 200000 electron events whereas the red distribution represents the detected p.e. for the scaled (detected pion events $\times$ π/e ratio) pion events.
(e)-(h) False pion detection efficiency and electron detection inefficiency. The blue curve represents the electron inefficiency with respect to the p.e. threshold. The red curve represents the scaled (Eqn. 2 $\times$ π/e ratio) false pion detection efficiency with respect to the p.e. threshold. The point of intersection defines the optimal threshold cut.*
*refer to text for further detail

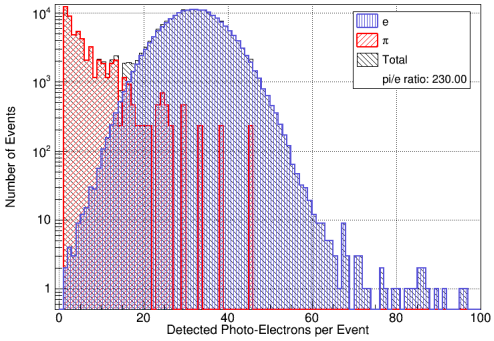

(a) C_4F_{10} @ $P = 0.50$atm & $p = 1.5$GeV/c

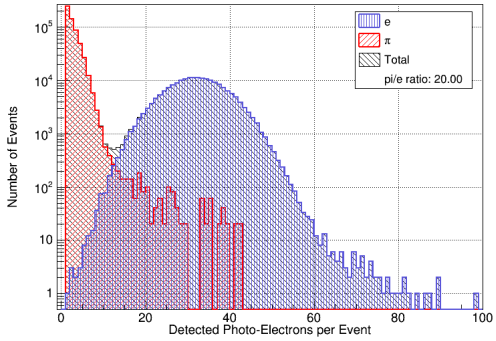

(b) C_4F_{10} @ $P = 0.50$atm & $p = 3$GeV/c

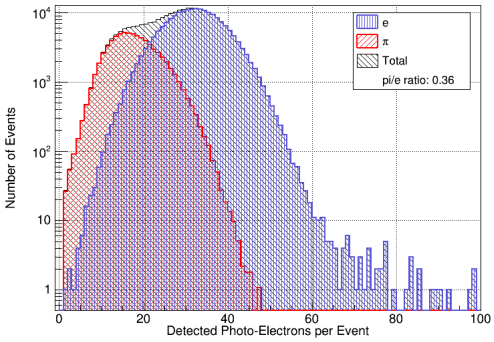

(c) C_4F_{10} @ $P = 0.50$atm & $p = 5$GeV/c

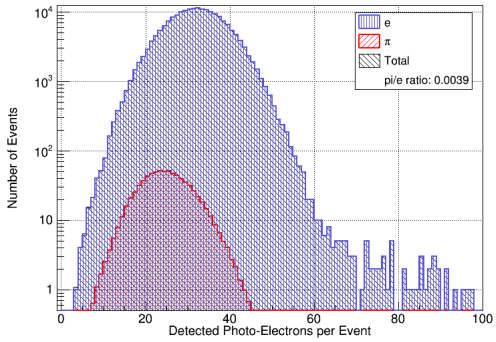

(d) C_4F_{10} @ $P = 0.50$atm & $p = 7$GeV/c

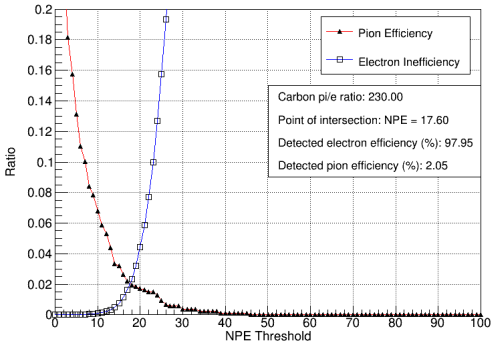

(e) C_4F_{10} @ $P = 0.50$atm & $p = 1.5$GeV/c

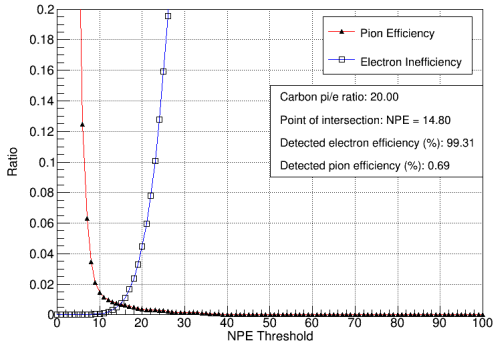

(f) C_4F_{10} @ $P = 0.50$atm & $p = 3$GeV/c

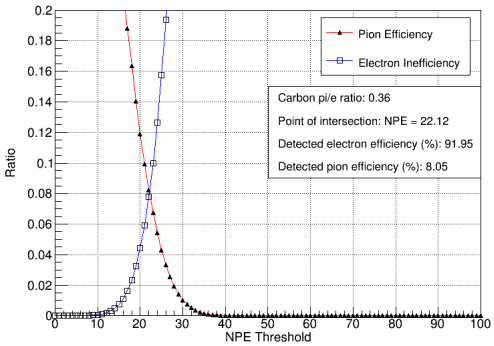

(g) C_4F_{10} @ $P = 0.50$atm & $p = 5$GeV/c

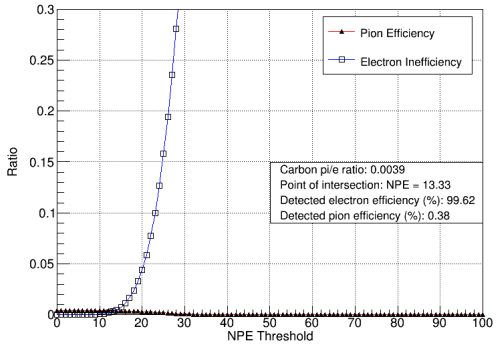

(h) C_4F_{10} @ $P = 0.50$atm & $p = 7$GeV/c

Figure 3: Refer to Fig. 2 for further information.

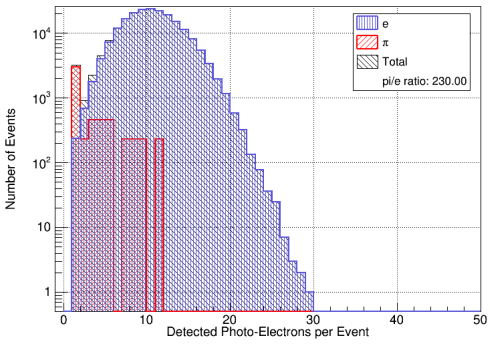

(a) CO_2 @ $P = 0.50$atm & $p = 1.5$GeV/c

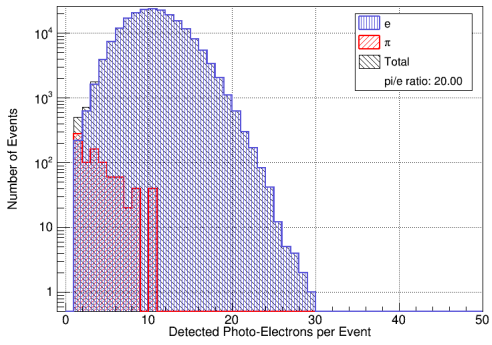

(b) CO_2 @ $P = 0.50$atm & $p = 3$GeV/c

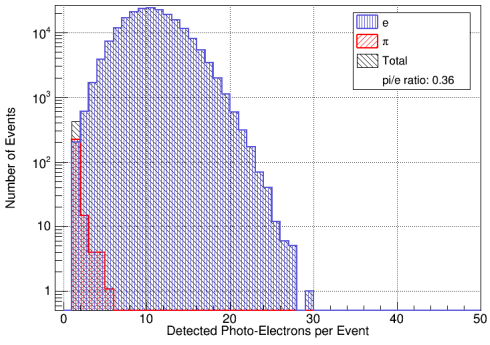

(c) CO_2 @ $P = 0.50$atm & $p = 5$GeV/c

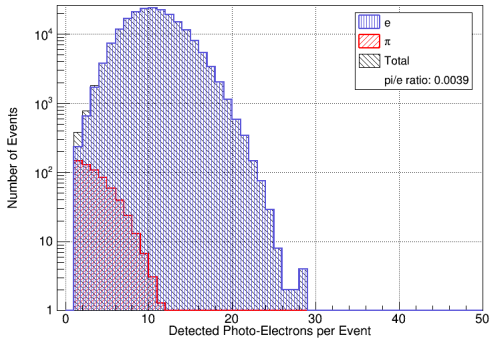

(d) CO_2 @ $P = 0.50$atm & $p = 7$GeV/c

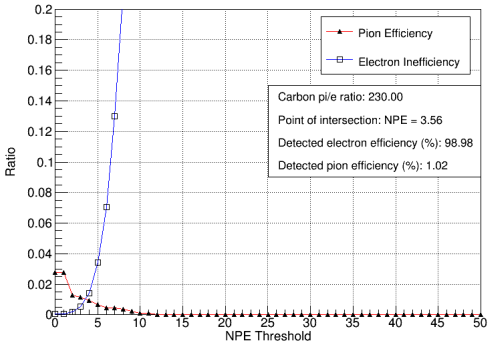

(e) CO_2 @ $P = 0.50$atm & $p = 1.5$GeV/c

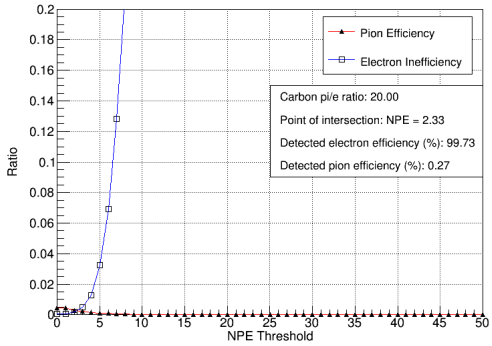

(f) CO_2 @ $P = 0.50$atm & $p = 3$GeV/c

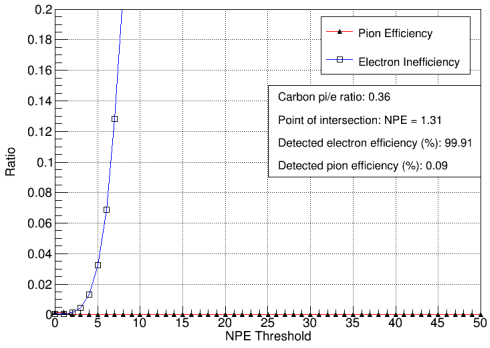

(g) CO_2 @ $P = 0.50$atm & $p = 5$GeV/c

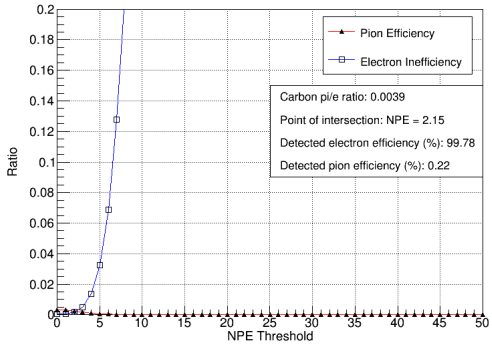

(h) CO_2 @ $P = 0.50$atm & $p = 7$GeV/c

Figure 4: Refer to Fig. 2 for further information.

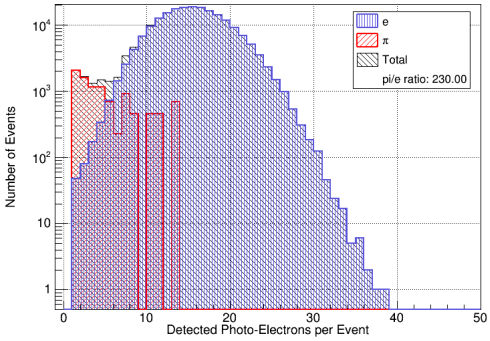

(a) CO_2 @ $P = 0.75$atm & $p = 1.5$GeV/c

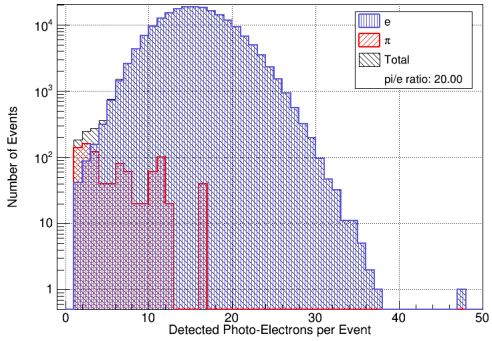

(b) CO_2 @ $P = 0.75$atm & $p = 3$GeV/c

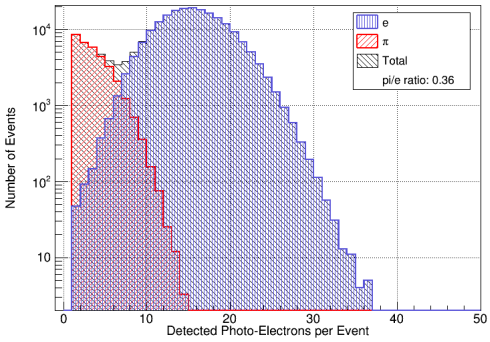

(c) CO_2 @ $P = 0.75$atm & $p = 5$GeV/c

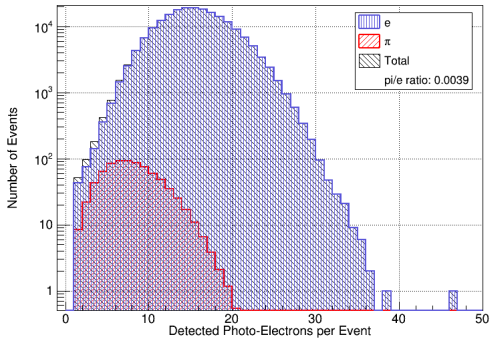

(d) CO_2 @ $P = 0.75$atm & $p = 7$GeV/c

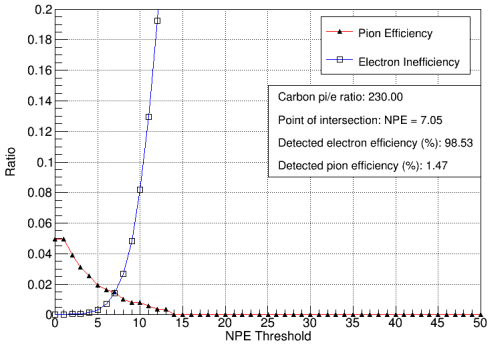

(e) CO_2 @ $P = 0.75$atm & $p = 1.5$GeV/c

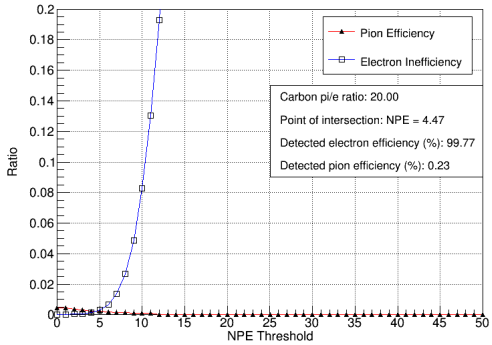

(f) CO_2 @ $P = 0.75$atm & $p = 3$GeV/c

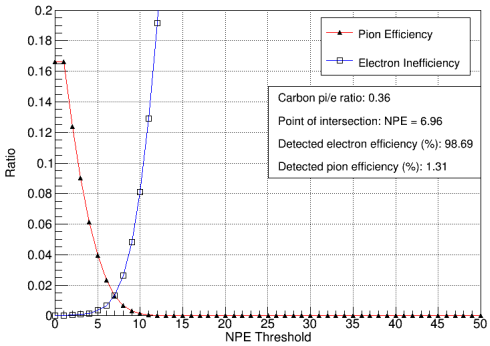

(g) CO_2 @ $P = 0.75$atm & $p = 5$GeV/c

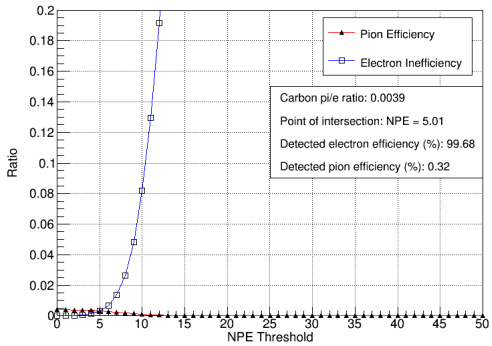

(h) CO_2 @ $P = 0.75$atm & $p = 7$GeV/c

Figure 5: Refer to Fig. 2 for further information.

These results suggest that CO_2 will provide a better combination of good electron identification efficiency and poor pion identification efficiency compared to C_4F_{10}. At low pressure (P = 0.25atm) and $p > 3$GeV/c, e/π separation is possible using C_4F_{10} although the number of detected p.e. per incident electron is less favourable. Overall, CO_2 has the greatest optimized performance at P = 0.50atm and a threshold cut at 3.6 p.e. This yields a detected electron efficiency greater than 98.98% and a false pion detection efficiency less than 1.02% for all simulated momenta. All recommended HGC operating pressures presented in this report are based on the assumption of a π/e production ratio of $\pi/e = \{230, 20, 0.36, 0.0039\}$ at the simulated momenta of $p = \{1.5\text{GeV/c}, 3.0\text{GeV/c}, 5.0\text{GeV/c}, 7.0\text{GeV/c}\}$ respectively. It is recommended to contact Dr. Garth Huber prior to setting the detector pressure.